Analysis of diverse optimisation algorithms in breast cancer detection

K. Senthil Kumar*

Department of EEE,
University College of Engineering Arni,
Arni, 632326, Tamil Nadu, India
Email: kslksenthil@gmail.com
*Corresponding author

K. Venkatalakshmi

Department of ECE,
University College of Engineering Tindivanam,
Melpakkam, 604001, Tindivanam, Tamil Nadu, India
Email: venkata_krish@yahoo.com

K. Karthikeyan

Department of ECE,
University College of Engineering Arni,
Arni, 632326, Tamil Nadu, India
Email: kuna.karthi@gmail.com

A. Jasiya Jabeen

University College of Engineering Tindivanam,
Melpakkam, 604001, Tindivanam, Tamil Nadu, India
Email: krishanth.green@gmail.com

Abstract: Breast cancer is a widespread problem faced by the women in recent years. It is highly essential to detect the breast cancer at an early stage to save lives. Image segmentation technique is used to segment the mistrustful masses from an ultrasound image of the breast. This work focuses on implementation and analysis of various optimisation algorithms in detecting mistrustful masses in the given ultrasound image of the breast. In preprocessing the speckle noise is reduced by using the median filter and contrast is improved by using adaptive histogram equalisation. Particle swarm optimisation, chaotic particle swarm optimisation (CPSO), k-medoids clustering, fuzzy c-means and k-means clustering are used in our work. A comparative analysis has been done using MATLAB and, it is proved that the CPSO has the best result among the others. The accuracy and dice similarity coefficient of the CPSO based method is 93.5793 and 0.8735 respectively.

Keywords: ultrasound image; median filter; Gaussian filter; histogram equalisation; particle swarm optimisation; CPSO; chaotic particle swarm optimisation; k-medoids; fuzzy c-means; k-means clustering; dice coefficient.

Reference to this paper should be made as follows: Senthil Kumar, K., Venkatalakshmi, K., Karthikeyan, K. and Jabeen, A.J. (2018) 'Analysis of diverse optimisation algorithms in breast cancer detection', *Int. J. Image Mining*, Vol. 3, No. 1, pp.4–21.

Biographical notes: K. Senthil Kumar is an Assistant Professor in the Department of EEE at the University College of Engineering Arni, Tamil Nadu, India. He completed his UG degree in 1997 and PG degree in 2000. He is presently doing PhD in part-time mode at Anna University, Chennai, India.

K. Venkatalakshmi is an Assistant Professor and HOD i/c in the Department of ECE at the University College of Engineering Arni, Tamil Nadu, India. She completed her Doctorate degree and presently guiding 10 research scholars. Her area of interest is image and video processing with optimisation algorithms.

K. Karthikeyan is a part time research scholar at Anna University, Chennai, India. He is presently working as Teaching fellow in the Department of ECE at the University College of Engineering Arni.

A. Jasiya Jabeen is a UG student of the University College of Engineering Tindivanam.

This paper is a revised and expanded version of a paper entitled 'Experimental study of optimization algorithms for breast cancer recognition by means of ultrasound images' presented at *International Conference on Informatics and Analytics (ICIA '16)*, Pondicherry Engineering College, Department of Computer Science and Engineering, 25–26 August, 2016.

1 Introduction

Diagnosis and analysis of the medical images is a crucial task in the recent medical treatment. Visual representations and numeric results extracted from a digital image of the interior body are highly useful in the analysis and diagnosis of diseases. The obtained information deal with human lives hence the accuracy is highly important. Preprocessing, segmentation, classification and feature extraction are the four major steps involved in image segmentation technique (Venkatalakshmi and Shalinie, 2007a). When there is no symptom or sign changes mammogram is used in detection and diagnosis of breast cancer. But in the mammogram, both cyst and tumour appear with white colour which reduces the segmentation accuracy, whereas in an ultrasound the cyst and tumour can be clearly differentiated and some breast changes which cannot be visualised in mammogram can be clearly visualised. Ultrasound is a low cost and non-ionising radiation method. In our work, we practically verified the segmentation accuracy in detection of breast cancer from an ultrasound image by using various optimisation methods. This work mainly focuses the analysis of the performance of particle swarm optimisation, chaotic particle swarm optimisation, k-medoids clustering, fuzzy c-means and k-means clustering with manual selection of cluster centres in breast cancer detection. In the preprocessing stage, we did a comparison between median and Gaussian filter in removing speckle noise from the ultrasound image. Adaptive histogram equalisation is also used to improve the contrast of the input image.

2 Literature review

Abdelwahed et al. (2015) used a CAD system for segmenting ultrasound image. A watershed transformation technique is implemented in their work to extract the region of interest from an ultrasound image. In this work, the problem of over segmentation has been solved. This work is more suitable to detect a tumour at an earlier stage. Kathiravan and Sundar Raj (2015) applied ridgelet transform to extract the statistical texture features. Venkatalakshmi and Shalinie (2004) proved that in multispectral image classification accuracy could be improved using ridgelet transform. Rose and Allwin (2013) suggested a tumour cut algorithm for segmentation of ultrasound images and it is evident in this work the detection rate is increased. Pate and Sinha (2010) implemented an adaptive k-means algorithm for early detection of breast cancer. Shareef (2014) shown that morphological watershed transform suits well for breast cancer detection from an ultrasound image.

3 Proposed method

A MATLAB based practical approach for the proposed work is revealed in Figure 1.

This work incorporates four stages viz. preprocessing, clustering, foreground extraction, and feature extraction. In preprocessing, we did noise removal and contrast enhancement on the input ultrasound breast image. The speckle noise present in the ultrasound image was removed using median and Gaussian filters. The image appearance is enhanced using adaptive histogram equalisation. A comparative analysis was done on the performance of noise removal between median and Gaussian filters. In the k-means clustering, the cluster centres are fixed using various optimisation algorithms viz. particle swarm optimisation, chaotic optimisation algorithm and k-medoids algorithm. The performance variations between the above-said algorithms were practically verified using MATLAB and compared. The k-means clustering with manual cluster centre selection was also shown to state the practical importance of optimisation algorithms.

3.1 Noise removal

The frequent possible noise occurrence in ultrasound is speckle noise (Yasmin et al., 2013). The resolution and contrast are reduced by the speckle noise. The boundaries and exact specification cannot be clearly observed in the presence of speckle noise. This complicates the diagnosis (Nicolae et al., 2009). The mathematical model of speckle noise is

$$g(m,n) = f(m,n) \times u(m,n) + e(m,n), \tag{1}$$

where

$g(m,n)$: image with speckle noise

$u(m,n)$: multiplicative component

$e(m,n)$: additive component

$f(m,n)$: input image.

The process flow diagram for the median filter is shown in Figure 2.

Figure 1 Schematic block diagram of proposed work

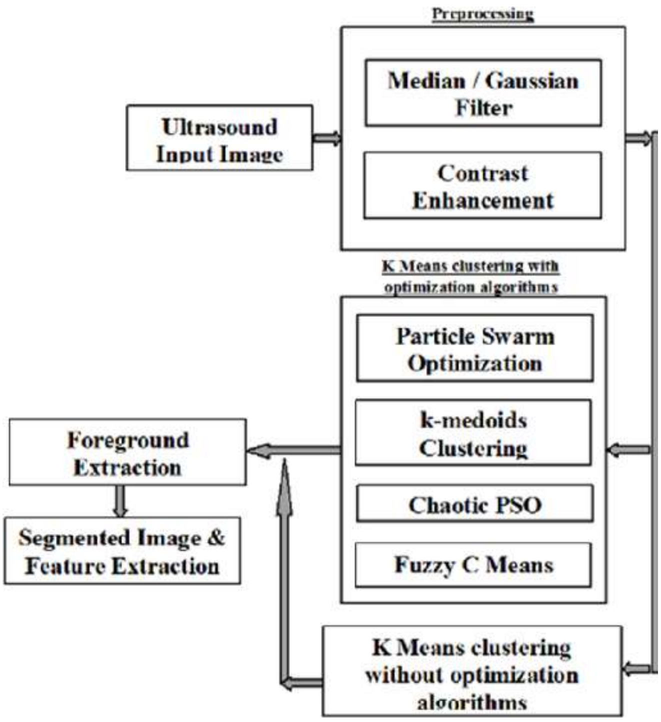

Figure 2 Process flow diagram for median filter

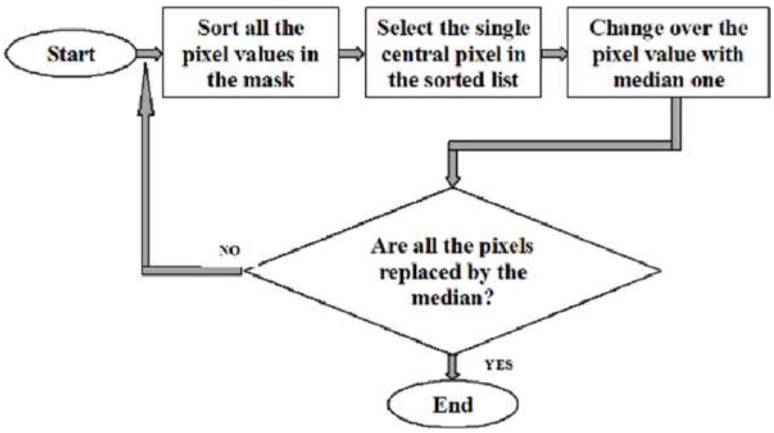

In our work comparison was done between the median and Gaussian filter in the elimination of speckle noise. The median filter has the superior feature than an average filter. Rather than the mean value, the median value of neighbouring pixels is used in the median filter. It is one of the best filters used in noise removal which removes the outliers without disturbing the sharpness of an image. The window in general in the median filter is of size 3×3 (Gupta, 2011). A convolution based Gaussian kernel is used in the Gaussian filter (Chandel and Gupta, 2013). The mathematical model of two-dimensional Gaussian functions is

$$G(x, y) = \frac{1}{2\pi\sigma^2} e^{-\frac{x^2+y^2}{2\sigma^2}}, \tag{2}$$

where the σ is the standard deviation.

The process flow diagram of the Gaussian filter is shown in Figure 3.

Figure 3 Process flow diagram for Gaussian filter

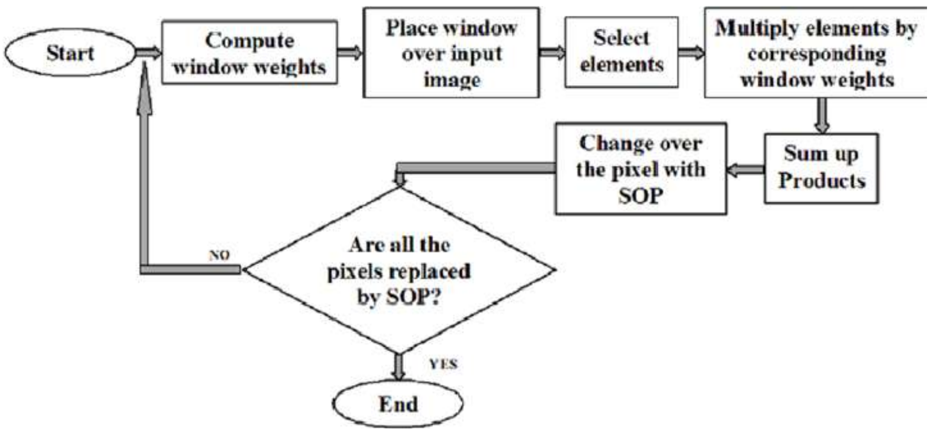

3.2 Contrast enhancement

It is essential to improve the visual appearance of a medical image to view the edges and excellent specifications clearly. In our work, we used adaptive histogram equalisation to increase the contrast of the input ultrasound image (Cheng et al., 2009). This is a mapping technique applied to all pixels in about its rank in the pixel nearby.

3.3 Image segmentation

Extracting some meaningful information from a digital image is called as image segmentation. It plays a vital role in medical imaging. The basics behind image segmentation are to group the pixels into two or more groups based on some features, particularly intensity. Plenty of methods are available to do this process out of that k-means clustering is one of the efficient methods. In k-means clustering, the optimum cluster centres are selected using optimisation algorithms. In our work, we used particle swarm optimisation (Guo et al., 2008; Venkatalakshmi et al., 2008), chaotic particle swarm optimisation and k-medoids clustering.

3.3.1 Particle swarm optimisation

Particle swarm optimisation is a metaheuristic algorithm used efficiently in medical image analysis. It mimics the social behaviour of the birds searching for food. The fundamental idea of PSO is sharing and communicating the information (Tandan et al., 2014). In this approach, each particle has initial position and velocity. Based on the fitness value, the velocity and position are updated (Kumar et al., 2015) and (Venkatalakshmi and Shalinie, 2005). The relevant two equations in PSO to update the position and velocity are,

$$v(t+1) = v(t) + c_1 r_1 [p_{\text{best}}(t) - x(t)] + c_2 r_2 [g_{\text{best}}(t) - x(t)] \tag{3}$$

$$x(t+1) = x(t) + v(t+1), \tag{4}$$

where r_1, r_2 are random numbers; the acceleration coefficients c_1 and c_2 are two positive constants. PSO needs a minimum number of iterations to converge towards an optimum. It has simple parameters, and there is no crossover and mutation. The success of PSO relies on the fitness function. In our work, we used the following fitness function.

$$\text{Maximise}\, f = \sum_{i=1}^{n} \frac{\text{Inter cluster distance}}{\text{Intra cluster distance}}, \tag{5}$$

where

n: number of clusters

The process flow diagram for the PSO algorithm is shown in Figure 4.

Figure 4 Process flow diagram for the PSO algorithm

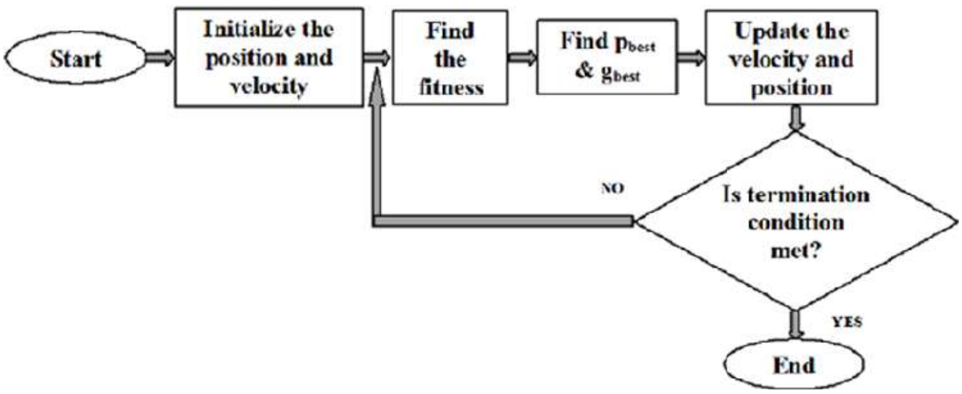

3.3.2 k-medoids clustering

k-medoids clustering aims to reduce the distance between the cluster centres to each pixel. *'k' numbers of mutually exclusive groups are formed by partitioning data in k-means (Venkatalakshmi and* Shalinie*, 2007b;* Venkatalakshmi et al., *2007)* and *k-medoids (Park and Jun, 2009)*. The k-medoids algorithm is based on k-means (Venkatalakshmi et al., 2008) and Medoidshift algorithm. It is more robust to noise and outliers because it minimises the sum of pair wise dissimilarities. The process flow diagram for the k-medoids algorithm is shown in Figure 5.

Figure 5 Process flow diagram for the k-medoids algorithm

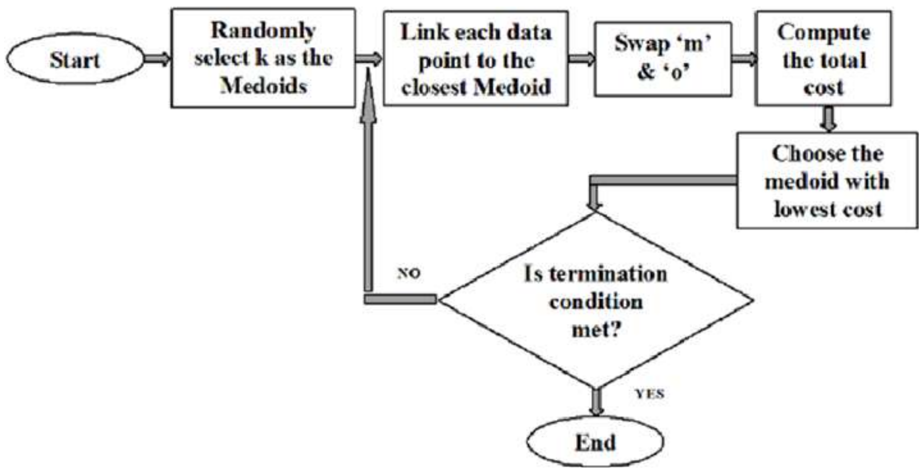

3.3.3 Chaotic particle swarm optimisation

Chaotic particle swarm optimisation (CPSO) exerts chaotic perturbation on global best which prevent the particle from premature convergence. In particle swarm optimisation, the convergence velocity gets reduced in later searches, and there is no guaranteed first solution. This shortfall is filled with chaotic particle swarm optimisation (Shang and Yang, 2006; Suganthan, 1999). A nonlinear system similar to random process and complex behaviour is called chaotic. The global convergence is improved by a logistic map with the following equations.

$$C_r(t+r) = k \times C_r(t) \times (1 - C_r(t)), \tag{6}$$

where

C_r: chaotic variable

k: control parameter.

The velocity update equation can be formulated as (Ye et al., 2012),

$$v(t+1) = v(t) + C_r[p_{\text{best}}(t) - x(t)] + (1 - C_r)[g_{\text{best}}(t) - x(t)]. \tag{7}$$

This method avoids local minima and improves global convergence. The parameters r_1 and r_2 are modified by the logistic map in CPSO. The process flow diagram for the CPSO algorithm is shown in Figure 6.

3.3.4 Fuzzy c-means

Fuzzy c-means is one among the unsupervised clustering methods segregates data into subsets based on the individual data feature. The Fuzzy c-means algorithm is almost similar to the k-means algorithm (Sable, 2015). The k-means algorithm reduces the complexity in the objective function. In the Fuzzy c-means algorithm, the objective function has membership values w_{ij} and the fuzifier $m \in R$ measures the level of cluster fuzziness. For crisp segmentation, m is limited to 1. The segmentation results are based on the initial choice of weights. Fuzzy c-means has been a critical tool for image processing in segmenting objects in an image. The process flow diagram (Sable, 2015) for the fuzzy c-means algorithm is shown in Figure 7.

Figure 6 Process flow diagram for the CPSO algorithm

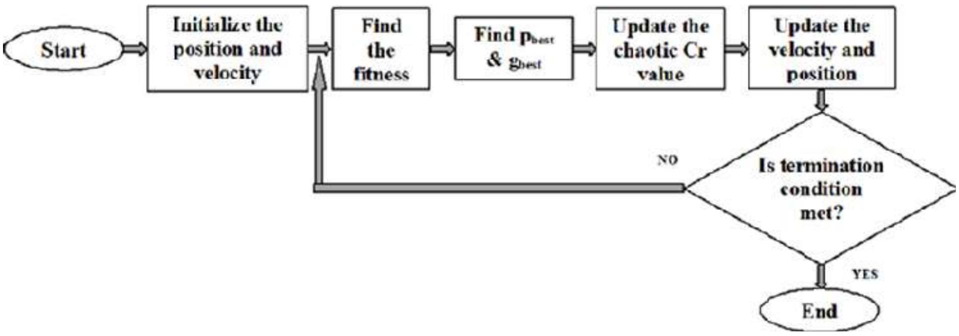

Figure 7 Process flow diagram for fuzzy c-means algorithm

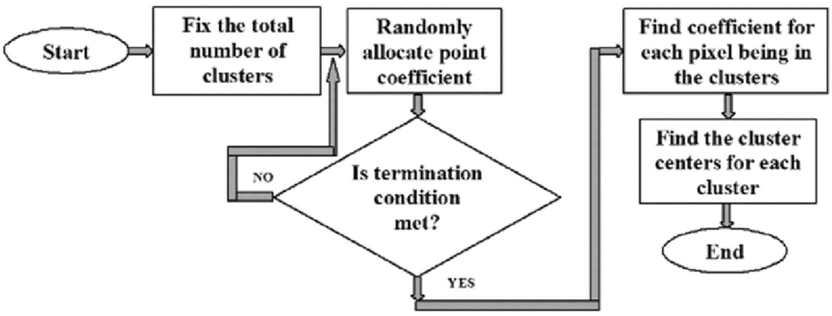

3.3.5 k-means clustering

K-means clustering segments the given set of data into k clusters in which each data belongs to a cluster with minimum mean. The distance between the cluster centres and to each pixel plays important role in this algorithm. The distance measure used here is Euclidean distance. The Euclidean distance between the cluster centres and the pixels are calculated. The pixel is assigned to a cluster with respect to the minimum value of Euclidean distance (Sable, 2015). The optimum cluster centres are identified with a certain number of repetitive iteration. The process flow diagram for the k-means clustering algorithm is shown in Figure 8.

A tumour is detected using the intensity-based thresholding method. The original segmented image is compared with the manually segmented image to find the statistical parameters as well as the performance measure of segmentation.

4 Performance measures

4.1 Speckle suppression index (SSI)

The ratio of coefficient of variance of a filtered image to the ratio of coefficient of variance of an input image is called as speckle suppression index. The ratio between standard deviation to mean of an image is called as the coefficient of variation. The mathematical expression of speckle suppression index (Wang et al., 2012) is,

$$\mathrm{SSI} = \frac{\sqrt{\mathrm{Var}(I_f)}}{\mathrm{Mean}(I_f)} \times \frac{\mathrm{Mean}(I_o)}{\sqrt{\mathrm{Var}(I_o)}}, \tag{8}$$

where

I_f: image after noise reduction

I_o: noisy image.

The value lesser than unity and lowest indicates that the filtered image has minimum speckle noise with improved quality.

Figure 8 Process flow diagram for the k-means algorithm

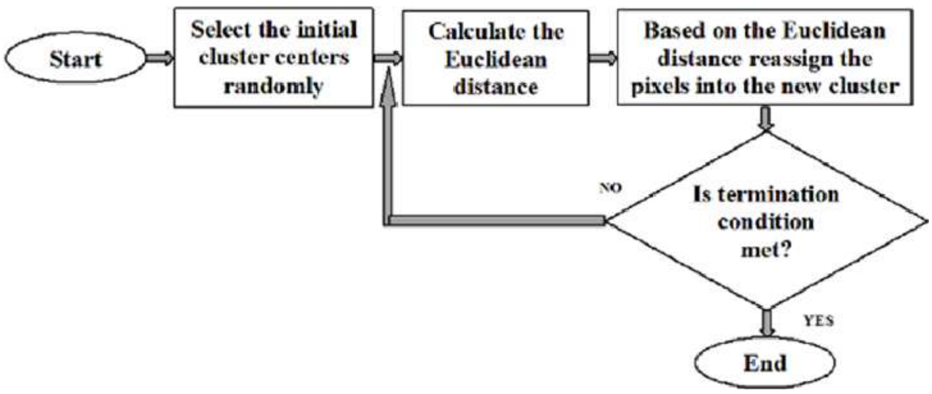

4.2 *Speckle suppression and mean preservation index (SMPI)*

If there is an overestimation of the average value the SSI will not be considered as a reliable measure. The mean preservation index is used under these circumstances. It is defined as (Wang et al., 2012),

$$\mathrm{SMPI} = Q \times \frac{\sqrt{\mathrm{Var}(I_f)}}{\sqrt{\mathrm{Var}(I_o)}}, \tag{9}$$

where Q can be defined as,

$$Q = 1 + \left|\mathrm{Mean}(I_0) - .(I_f)\right|. \tag{10}$$

The value lesser than unity and lowest indicates that the filtered image has minimum speckle noise with improved quality.

4.3 *True positive (tp)*

When a patient has the disease and the test result is positive it is called true positive. This parameter defines existing one as existing. In this case, the pixels segmented correctly as foreground and the true positive should be high. When we compare the binary input image with the binary ground truth image for each pixel, the total number of matches of foreground (1) is called true positive. The sensitivity otherwise true positive rate (Carsten Schwenke and Schering, 2014) in image segmentation is defined as,

$$tpr = \frac{tp}{tp + fn}. \tag{11}$$

4.4 True negative (tn)

When a patient has no disease and the test result is negative is called true negative. This parameter defines non-existing one as non-existing. In this case, the pixels segmented correctly as background and the true negative should be high. When we compare the binary input image with the binary ground truth image for each pixel, the total number of matches of background (0) is called true negative. The specificity otherwise true negative rate (Schwenke and Schering, 2014) in image segmentation is defined as,

$$tnr = \frac{tn}{tn + fp}. \tag{12}$$

4.5 False positive (fp)

When a patient has no disease and the test result is positive is called false positive. This parameter defines non-existing one as existing. In this case, the pixels wrongly segmented as foreground and the false positive should be low. When we compare the binary input image with the binary ground truth image for each pixel, the total number of mismatches for foreground is called false positive. The false positive rate (Schwenke and Schering, 2014) in image segmentation is defined as,

$$fpr = \frac{fp}{fp + tn}. \tag{13}$$

4.6 False negative (fn)

When a patient has the disease and the test result is negative it is called false negative. This parameter defines existing one as non-existing. In this case, the pixels are wrongly segmented as background, and the false negative should be low. When we compare the binary input image with the binary ground truth image for each pixel, the total number of mismatches for the background is called false negative. The false negative rate (Schwenke and Schering, 2014) in image segmentation is defined as,

$$fnr = \frac{fn}{fn + tp}. \tag{14}$$

4.7 Accuracy

Accuracy is a degree of measure to state the correctness of a process. In image segmentation, the accuracy is defined as,

$$\text{Accuracy} = \frac{tp + tn}{tp + tn + fp + fn}. \tag{15}$$

When the true positive and true negative are high, and the false positive and false negative are low, it indicates the image is correctly segmented as foreground and background, and the accuracy will become high and almost near to 1.

4.8 Dice coefficient

Dice coefficient otherwise called as overlap index is used to measure the similarity between two results. It is twice the ratio between a number of non-zero elements in the intersection of input and ground truth images to the total number of non-zero elements in data and the number of non-zero elements in the ground truth image. The dice coefficient is always greater than the Jaccard coefficient (Schwenke and Schering, 2014).

$$\text{Dice Coefficient} = \frac{2 \times tp}{tp + fp + fn}. \tag{16}$$

5 Experimental results

5.1 Comparative analysis of filter performance

Table 1 depicts the performance evaluation comparison between the median and Gaussian filters.

Table 1 Comparative analysis of filters

Parameter	*Median filter*	*Gaussian filter*
SSI	0.80	0.82
SMPI	6.31	7.90

The variations of SSI and SMPI are represented in Figures 9 and 10 graphically. The SSI and SMPI values of the median filter are minimum than the Gaussian filter. From this, it is evident that the median filter produces a better result than the Gaussian in the elimination of speckle noise. The resultant images after filtering along with input image and the output image after contrast enhancement are shown in Figure 11.

5.2 Performance evaluation of segmentation

The image after clustering and the region of interest are shown in Figures 12–16.

Figure 9 Graphical variation of SSI (see online version for colours)

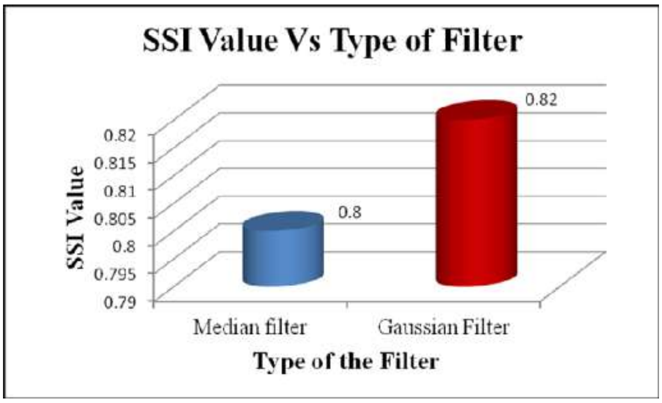

Figure 10 Graphical variations of SMPI (see online version for colours)

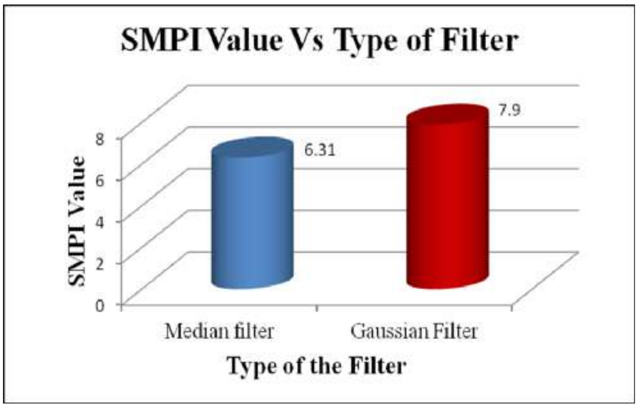

Figure 11 Images after preprocessing: (A1) input; (A2) median filter output; (A3) Gaussian filter output and (A4) contrast enhanced image

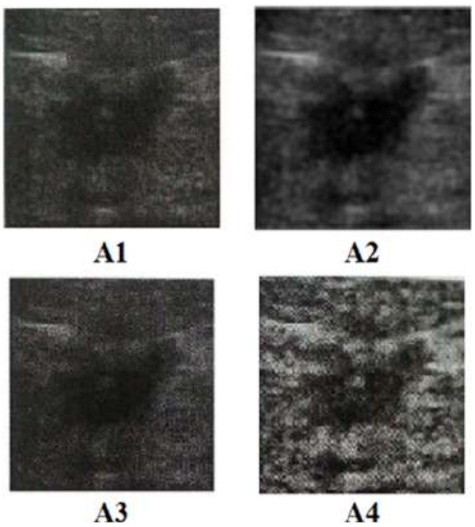

Figure 12 Input and output images using PSO: (A1) PSO clustered image and (A2) segmented image (ROI)

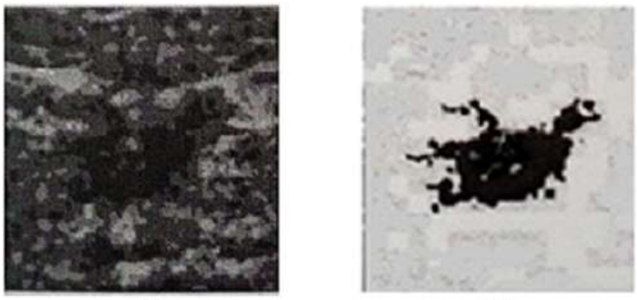

A1 A2

Figure 13 Input and output images using k-medoids: (A1) k-medoids clustered image and (A2) segmented image (ROI)

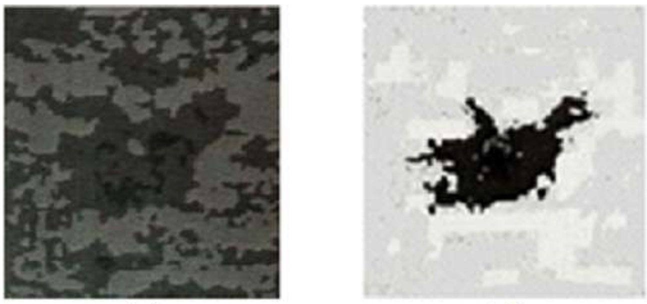

A1 A2

Figure 14 Input and output images using CPSO: (A1) CPSO clustered image and (A2) segmented image (ROI)

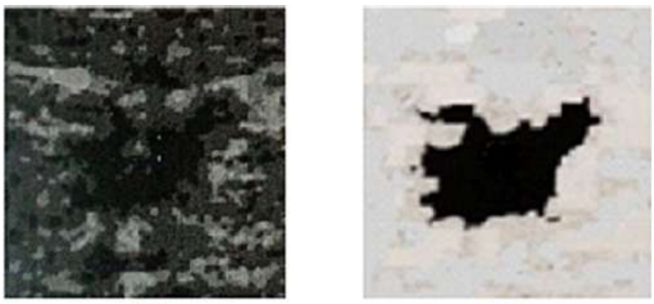

A1 A2

The performance level of the particle swarm optimisation, k-medoids clustering, chaotic particle swarm optimisation, fuzzy c-means and k-means clustering are compared with the help of true positive rate, true negative rate, false positive rate, false negative rate, accuracy and dice coefficient. The observations on true positive and true negative rate are tabulated in Table 2, and the graphical variations are shown in Figure 17.

Figure 15 Input and output images using fuzzy c-mean: (A1) fuzzy c-means clustered image and (A2) segmented image (ROI)

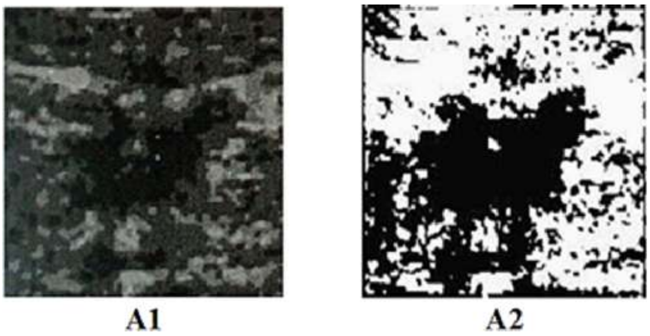

Figure 16 Input and output images using k-means: (A1) k-means clustered image and (A2) segmented image (ROI)

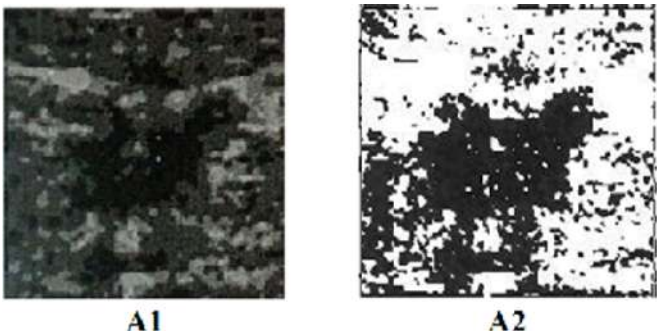

Table 2 Comparison of true positive and true negative rate

Algorithm	*True positive rate*	*True negative rate*
PSO	80.4143	83.6145
k-medoids	80.6055	83.7485
CPSO	93.3673	93.7788
Fuzzy c-means	92.9612	69.6275
k-means	88.6850	70.1822

The observations on false positive and false negative rate are tabulated in Table 3, and the graphical variations are shown in Figure 18.

Table 3 Comparison of true positive and true negative rate

Algorithm	*False positive rate*	*False negative rate*
PSO	16.3855	19.5857
k-medoids	16.2515	19.3945
CPSO	6.2212	6.6327
Fuzzy c-means	30.3725	7.0388
k-means	29.8178	11.3150

Figure 17 Comparative analysis of TP &TN rate (see online version for colours)

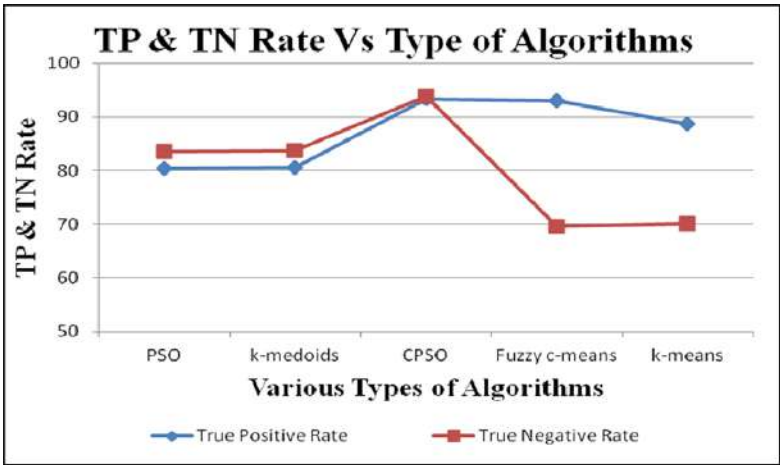

Figure 18 Comparative analysis of FP &FN rate (see online version for colours)

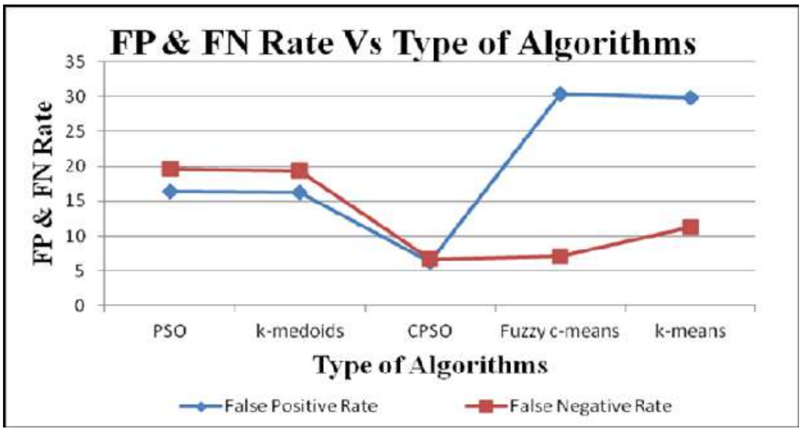

The observation on Dice coefficient is tabulated in Table 4, and the graphical variations are shown in Figure 19.

Table 4 Comparative analysis of accuracy

Algorithm	*PSO*	*k-medoids*	*CPSO*	*Fuzzy c-means*	*k-means*
Dice Coefficient	0.8041	0.8067	0.8737	0.8408	0.8366

The observation about accuracy is tabulated in Table 5, and the graphical variations are shown in Figure 20.

Table 5 Comparative analysis of accuracy

Algorithm	*PSO*	*k-medoids*	*CPSO*	*Fuzzy c-means*	*k-means*
Accuracy	82.1554	82.3134	93.5793	81.7333	80.5630

Figure19 Comparative analysis of Dice coefficient (see online version for colours)

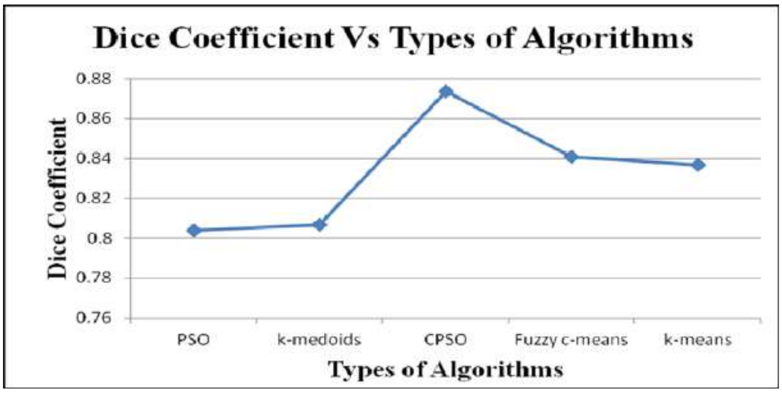

Figure 20 Comparative analysis of dice coefficient (see online version for colours)

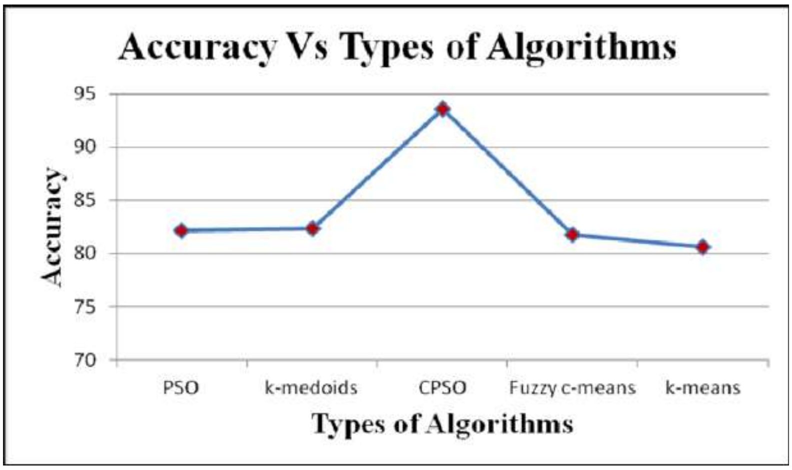

For proper segmentation, true positive and true negative should be high at the same time false positive and false negative should be low. From Table 2 and Figure 17, it is observed that the true positive and true negative rates of CPSO are 93.3673 and 93.7788, respectively. This has highest values compared to PSO, k-medoids, Fuzzy c-means and k-means clustering algorithms. At the same time, it is eminent from the Table 3 and Figure 18 that the false positive and false negative rates of CPSO are 6.2212 and 6.6327, respectively. This has lowest values compared to PSO, k-medoids, Fuzzy c-means and k-means clustering algorithms. These results clearly represent that the CPSO algorithm has superior characteristics than PSO, K-medoids, Fuzzy c-means and k-means clustering algorithms. From Table 4 and Figure 10, it is clear that the dice coefficient of CPSO is 0.8735 comparatively high about PSO, k-medoids, Fuzzy c-means and k-means clustering algorithms. It shows that the manual segmentation result agrees 87.35% with segmentation using CPSO. From Table 5 and Figure 20, it is clear that the CPSO algorithm has the highest accuracy of 93.5731%. This is greater than the current watershed transformation based segmentation method (Shareef, 2014).

6 Conclusion

In this work, the breast cancer is detected using PSO, k-medoids, CPSO, Fuzzy c-means and k-means clustering algorithms. This work relies on effective de-noising and enhancement for medical ultrasound image. The simple k-means clustering is used in our algorithm with manual cluster centre selection to depict that the optimisation algorithm is essential in the selection of cluster centres. The performance measures for segmentation and statistical parameters are also measured to calculate the accuracy. It is observed that the true positive and true negative rates of CPSO are 93.3673 and 93.7788, respectively and the false positive and false negative rates of CPSO are 6.2212 and 6.6327, respectively. Further, it is clear that the dice coefficient of CPSO is 0.8735 the manual segmentation result agrees 87.35%. It is practically proved that the CPSO algorithm with the median filter in preprocessing stage yields an optimum result compared to the earlier and other methods.

References

Abdelwahed, N.M.A., Eltoukhy, M.M. and Wahed. M.E. (2015) 'Computer aided system for breast cancer diagnosis in ultrasound images', *Journal of Ecology of Health and Environment*, Vol. 3, No. 3, pp.71–76.

Chandel, R. and Gupta, G. (2013) 'Image filtering algorithms and techniques: a review', *International Journal of Advanced Research in Computer Science and Software Engineering*. Vol. 3, No. 10, ISSN: 2277 128X.

Cheng, H.D., Shan, J., Ju, W., Guo, Y. and Zhang, L. (2009) 'Automated breast cancer detection and classification using ultrasound images: a survey', *Pattern Recognition*, Vol. 43, No. 1, pp.299–317.

Guo, Y., Cheng, H.D., Tian, J. and Zhang, Y. (2008) 'A novel approach–breast ultrasound image segmentation based on the characteristics of breast tissue and particle swarm optimization', *Proceedings of the 11th Joint Conference on Information Sciences*, Published by Atlantis Press, Harbin Institute of Technology, Shenzhen, China.

Gupta, G. (2011) 'Algorithm for image processing using improved median filter and comparison of mean, median and improved median filter', *International Journal of Soft Computing and Engineering*, Vol. 1, No. 5, ISSN: 2231-2307.

Kathiravan, M. and Sundar Raj, M. (2015) 'Ridgelet based feature extraction for breast cancer detection using ultrasound images', *Indian Journal of Science and Technology*, Vol. 8, No. 31, http://dx.doi.org/10.17485/ijst/2015/v8i31/87752

Kumar, K.S., Venkatalakshmi, K., Karthikeyan, K. and Kathirkamasundari. P. (2015) 'An efficient method for segmenting digital image using a hybrid model of particle swarm optimization and artificial bee colony algorithm', *International Journal of Applied Engineering Research*, Vol. 10, pp.444–449.

Nicolae, M., Moraru, L. and Gogu, A. (2009) 'Speckle noise reduction of ultrasound images', *Medical Ultrasonography an International Journal of Clinical* Imaging, Vol. 11, pp.50, 51.

Park, H-S. and Jun, C-H. (2009) 'A simple and fast algorithm for K-medoids clustering', *Expert Systems with Applications*, Vol. 36, No. 2, pp.3336–3341.

Pate, B.C. and Sinha, G.R. (2010) 'An adaptive K-means clustering algorithm for breast image segmentation', *International Journal of Computer Applications*, 0975 – 8887 Volume 10– N, http://dx.doi.org/10.5120/1467-1982

Rose, R.J. and Allwin, S. (2013) 'Computerized cancer detection and classification using ultrasound images: a survey', *International Journal of Engineering Research and Development*, e-ISSN: 2278-067X, p-ISSN: 2278-800X, Vol. 5, No. 7, pp.36–47.

Sable, S.D. (2015) 'Implementation and analysis of k- means and fuzzy c means clustering techniques', *Proceedings of 26th IRF International Conference*, 10 May, Pune, India, ISBN: 978-93-85465-09-3.

Schwenke, C. and Schering, A.G. (2014) *True Positives, True Negatives, False Positives, False Negatives*, This article was originally published online in 2007 in Wiley Encyclopedia of Clinical Trials, © John Wiley & Sons, Inc. and Republished in Wiley statsref: Statistics Reference Online, 2014. DOI: 10.1002/9781118445112.stat06783.

Shang, G. and Yang, J-Y. (2006) 'Research on chaos particle swarm optimization algorithm', *Pattern Recognition and Artificial Intelligence*, April, pp.267–270.

Shareef, S.R. (2014) 'Breast cancer detection based on watershed transformation', *International Journal of Computer Science Issues*, Vol. 11, No. 1, pp.237–245.

Suganthan, P.N. (1999) 'Particle swarm optimizer with neighborhood operator', *Proceedings of the 1999 Congress on Evolutionary Computation-CEC99 (Cat. No. 99TH8406)*, http://dx.doi.org/10.1109/cec.1999.785514

Tandan, A., Raja, R. and Chouhan, Y. (2014) 'Image segmentation based on particle swarm optimization technique', *International Journal of Science Engineering and Technology Research*, Vol. 3, No. 2, pp.257–260.

Venkatalakshmi, K. and Shalinie, S.M. (2004) 'Classification of multispectral images using neuro statistical classifier based on decision fusion and feature fusion', *Proceedings of the IEEE International Conference on Intelligent Sensing and Information Processing*, Chennai, pp.283–288. http://dx.doi.org/10.1109/icisip.2004.1287668

Venkatalakshmi, K. and Shalinie, S.M. (2005) 'Classification of multispectral images using support vector machines based on PSO and K-Means clustering', *Proceedings of IEEE International Conference on Intelligent Sensing and Information Processing*, pp.127–133, http://dx.doi.org/10.1109/icisip.2005.1529435

Venkatalakshmi, K. and Shalinie, S.M. (2007a) 'Multispectral image classification using support vector machines and neural networks based on intensity measures', *Proceedings of the National Conference on Advanced Communication Technologies*, pp.13–15, 13–19, 111.

Venkatalakshmi, K. and Shalinie, S.M. (2007b) 'Multispectral image classification using modified k-means clustering', *International Journal on Neural and Mass-Parallel Computing and Information Systems*, Prague, Vol. 17, No. 2, pp.113–120.

Venkatalakshmi, K., Praisy, P.A., Maragathavalli, R. and Shalinie, S.M. (2007) 'Multispectral image clustering using enhanced genetic k-means algorithm', *Information Technology Journal*, Vol. 6, No. 4, pp.554–560.

Venkatalakshmi, K., Praisy, P.A., Maragathavalli, R. and Shalinie, S.M. (2008) 'A customized particle swarm optimization for classification of multispectral imagery based on feature fusion', *The International Arab Journal of Information Technology*, Vol. 5, No. 4, pp.327–333.

Wang, X., Ge, L. and Li, X. (2012) 'Evaluation of filters For EnvisatAsar speckle suppression in pasture area', *ISPRS Annals of the Photogrammetry. Remote Sensing and Spatial Information Sciences, Vol. I-7, 2012 XXII ISPRS Congress*, 25 August – 01, Melbourne, Australia, http://dx.doi.org/10.5194/isprsannals-i-7-341-2012

Yasmin, M., Sharif, M. and Mohsin, S. (2013) 'Survey work on diagnosis of breast cancer using image processing techniques', *Research Journal of Recent Sciences*, ISSN 2277-2502, Vol. 2, No. 10, pp.88–98.

Ye, Z., Hu, Z., Lai, X. and Chen, H. (2012) 'Image segmentation using thresholding and swarm intelligence', *Journal of Software*, Vol. 7, No. 5, http://dx.doi.org/10.4304/jsw.7.5.1074-1082